JOINT CONFERENCE PROCEEDINGS
7th International Conference on Urban Earthquake Engineering (7CUEE) &
5th International Conference on Earthquake Engineering (5ICEE)
March 3-5, 2010, Tokyo Institute of Technology, Tokyo, Japan

BAYESIAN NETWORK FOR INFRASTRUCTURE SEISMIC RISK ASSESSMENT: CHALLENGES AND OPPORTUNITIES

Michelle T. Bensi[1)], Armen Der Kiureghian[2)], and Daniel Straub[3)]

1) Doctoral Candidate, Department of Civil & Environmental Engineering, University of California, Berkeley, USA
2) Taisei Professor of Civil Engineering, Department of Civil & Environmental Engineering, University of California, Berkeley, USA
3) Associate Professor, Engineering Risk Analysis Group, Technical University Munich, Germany
mbensi@berkeley.edu, adk@ce.berkeley.edu, straub@era.bv.tum.de

Abstract: An overview of recent efforts directed at developing a probabilistic decision-support system (DSS) for seismic infrastructure risk assessment and management is presented. The DSS is based on a Bayesian network (BN) framework which is particularly well-suited for the proposed application. BNs are graphical and intuitive, facilitate information updating, can be used for identification of critical components within a system, and can be extended by decision and utility nodes to solve decision problems. In particular, the facility for information updating renders the BN an ideal tool for post-event infrastructure risk assessment and decision support. However, BNs have several limitations that must be addressed to make them a viable tool in the suggested context. Some of these challenges and proposed solutions are described in this paper.

1. INTRODUCTION

Civil infrastructure systems are the backbones of modern societies yet they remain vulnerable to a wide-variety of natural and man-made hazards. In many regions of the world earthquakes pose the dominant risk to infrastructure systems. However, through sound engineering and decision-making it is possible to mitigate these risks. There are three distinct phases during which seismic risk assessment and management decisions must be made: (1) pre-event, (2) immediate post-event, and (3) longer-term post-event. In the phase prior to the occurrence of an earthquake, it is necessary to assess risks by identifying critical components and bottlenecks in the system, and then take actions to minimize the risk exposure, e.g. retrofit/replace components, implement an optimal inspection/maintenance schedule, modify system configuration. In the phase immediately following an earthquake, decisions must be made to reduce the severity of post-event consequences. Often, at this stage, emphasis is placed on life safety and restoration of critical services. Post-event decisions include the dispatching of rescue, inspection, and repair crews as well as decisions to open or close facilities. These decisions are made under the competing demands to maintain operability (to prevent revenue loss) while not sacrificing safety (to avoid deaths and injury, as well as liability). This decision-phase is characterized by an environment in which information is both uncertain and quickly evolving in time. Sources of information at this phase may include ground motion (GM) intensity measurements, structural health monitoring sensors, inspection results, and even observations reported by citizens and facility employees. Finally, in the longer-term post-earthquake recovery phase, it is necessary to take actions to minimize long-term economic consequences from the event, e.g. optimal prioritization of replacement and retrofitting of damaged facilities. Additionally, hazard and system models must be updated based on knowledge gained from the earthquake.

With the above motivation in mind, we are working toward the development of a probabilistic decision-support system (DSS) for seismic infrastructure risk assessment and management. Ultimately, the DSS will aid decision-making during each of the aforementioned phases. To date, our efforts have focused primarily on a post-earthquake DSS able to incorporate uncertain and time-evolving information from a variety of sources. We utilize a Bayesian Network (BN) framework for the DSS because it is particularly well-suited for the proposed application. This paper provides an overview of the BN models developed for this purpose.

The paper begins with a brief introduction to BNs. Next, an overview of recent work towards the development of the DSS is presented. Components of the proposed BN framework include: (1) a seismic demand model of ground motion intensity as a spatially distributed random field accounting for finite fault rupture and directivity effects, (2) models of performance for both point-site and distributed components, (3) models of system performance, and (4) the extension of the BN to include decision and utility nodes to aid post-earthquake decision-making. Like other computational methods, BNs are not without shortcomings. In particular, calculations in BNs can be highly demanding of computer memory. Throughout the paper, work done to address this limitation is described.

2. BRIEF ON BAYESIAN NETWORKS

2.1 Motivation for using Bayesian networks

A BN is a probabilistic graphical model that represents a set of random variables and their probabilistic dependencies. The variables may represent demand or capacity values, or the states of components and systems. BNs are graphical and intuitive, facilitate information updating, can be used for identification of critical components within a system, and can be extended by decision and utility nodes to solve decision problems. In particular, the facility for information updating renders the BN an ideal tool for infrastructure risk assessment and decision support. Evidence on one or more variables (e.g. observed component capacities, demands, or component/system states) is entered into the BN and this information propagates throughout the network to provide an up-to-date probabilistic characterization of the performance of the infrastructure system in light of the new observations. This dynamic system representation is particularly critical for post-event, near-real time applications when the available information is uncertain and rapidly evolves with time.

2.2 Brief Introduction to Bayesian Networks

A BN is a directed acyclic graphical model consisting of a set of nodes representing random variables and a set of links representing probabilistic dependencies. Typically, links represent causal relationships. Consider the simple BN shown in Figure 1 modeling five random variables $\mathbf{X} = \{X_1, \dots X_5\}$ and their probabilistic relationships. For example, the random variable X_3 is probabilistically dependent on variables X_1 and X_2, as represented by arrows going from nodes X_1 and X_2 to node X_3. In the BN terminology, X_3 is a *child* of X_1 and X_2, while X_1 and X_2 are the *parents* of X_3. Additionally, X_4 is defined conditionally on its parent node X_1 and X_5 is defined conditionally on X_4. Each node is associated with a set of mutually exclusive collectively exhaustive states. To be able to utilize exact inference algorithms, it is generally necessary to discretize all continuous random variables in the BN (with the exception of continuous Gaussian nodes without discrete children). We will not address BNs with continuous nodes in this paper, but additional details can be found in Lauritzen (1992), Lauritzen & Jensen (2001), and Langseth (2009). For discrete nodes, probabilistic dependencies are encoded by attaching to each node a *conditional probability table* (CPT) providing the conditional probability mass function (PMF) of the random variable given each of the mutually exclusive states of its parents. . For random variables without parents (e.g. X_1 and X_2), a marginal probability table is assigned.

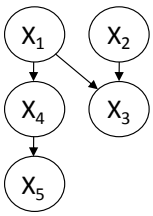

Figure 1: A simple BN

The ability to model a problem using conditional distributions is convenient in civil engineering applications, where often only conditional relationships are available, e.g. typically we may know the probability of a load exceeding a specific value *given* an event of a certain size, or the probability of damage *given* a particular demand value. The joint distribution of all random variables in the BN, **X**, is constructed as a product of the conditional distributions as

$$p(\mathbf{X}) = \prod_{i=1}^{n} p(x_i | pa(x_i)) \quad (1)$$

where $pa(x_i)$ is the set of parents of node X_i, $p(x_i | pa(x_i))$ is the CPT of X_i and n is the number of random variables (nodes) in the BN. Thus, for the BN in Figure 1, the joint PMF is

$$p(x_1, x_2, x_3, x_4, x_5) = \\ = p(x_5|x_4)p(x_4|x_1)p(x_3|x_1, x_2)p(x_1)p(x_2) \quad (2)$$

BNs are useful for answering probabilistic queries when one or more variables are observed. That is, BNs efficiently compute the conditional distribution of any subset $\mathbf{X}'$ of the variables in the BN given observations (or evidence) on any other subset $\mathbf{X}^e$ of the variables . The ease with which BNs facilitate the calculation of the conditional distribution $p(\mathbf{X}'|\mathbf{X}^e)$ is the main feature that makes the BN framework ideally suited for the proposed application. For example, suppose observations have been made on nodes X_3 and X_5 in Figure 1 and we are interested in computing the conditional distribution $p(X_2|X_3 = x_3, X_5 = x_5)$. This quantity can be computed by first marginalizing the joint distribution in (2) to obtain the joint distributions over the subsets of the variables:

$$p(x_2, x_3, x_5) = \sum_{x_1, x_4} p(x_1, \dots, x_5) \\ p(x_3, x_5) = \sum_{x_1, x_2, x_4} p(x_1, \dots, x_5) \quad (3)$$

The desired conditional distribution is then obtained as

$$p(x_2|x_3, x_5) = \frac{p(x_2, x_3, x_5)}{p(x_3, x_5)} \quad (4)$$

There are more efficient ways to do this calculation. Specifically, there are algorithms that facilitate probabilistic updating in BNs without repeated calculations over the joint distribution as demonstrated above. The reader is referred to Jensen & Nielson (2007) for additional details on probabilistic inference algorithms.

3. SEISMIC DEMAND MODEL

Infrastructure systems are typically distributed over a geographic region. As a result, they have a higher rate of exposure to hazard than single-site facilities and are subject to a wider range of hazards (e.g. ground shaking, ground deformation due to liquefaction and fault rupture). Furthermore, the ground motion intensity must be modeled as a spatially distributed random field to account for the statistical dependence between the seismic demand values at the locations of different components of the system.

In this section we introduce a BN model of the GM intensity as a spatially distributed random field. We focus here on hazard due to ground-shaking, but the framework is easily extended to other hazards. Models for predicting liquefaction-

induced ground deformation (lateral spreading, settlement) are currently under development.

Consider a system of n sites distributed over a geographic region in the vicinity of multiple faults. We now construct a BN predicting the distribution of GM intensity at each site for an earthquake occurring randomly on one of the faults. For each earthquake fault, there is a source-dependent distribution of magnitude and earthquake epicenter location. Furthermore, the rupture length on a fault is a function of earthquake magnitude and source characteristics (Wells & Coppersmith 1994). Figure 2 shows a BN model of these relationships. The node representing magnitude (M) is specified as a child of the source node (S_C), indicating that the probability of experiencing an earthquake of a certain magnitude differs based on the source. Similarly, S_c is a parent of the node modeling epicenter location (X_e). Node R_L, representing the rupture length, is a child of node M and node S_C.

To define the geometry of the geographic region of the infrastructure system, we use a fault specific local coordinate system. Consider an idealization of a fault as a straight line. A source-specific local coordinate system with the fault oriented along the x-axis and its left end located at the origin is shown in Figure 3. In this local coordinate system, the location of the epicenter (shown as a star in Figure 3) is defined by a point on the x-axis between 0 and F_L, where F_L is the length of the fault. The location of the rupture within the fault is defined as a function of the epicenter location and the rupture length. Let X_r denote the coordinate of the left end of the rupture. Assuming the length of the segment of the rupture to the left of the epicenter is uniformly distributed over the interval $[0, R_L]$, one can show that X_r is uniformly distributed within the interval

$$\left[X_e - \min(R_L, X_e)\,, X_e - \max\left(0, R_L - (F_L - X_e)\right)\right] \quad (5)$$

Thus, node X_r is a child of S_c, R_L, and X_e.

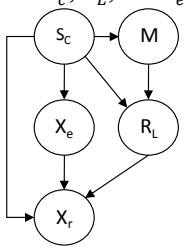

Figure 2: BN modeling rupture length and location as a function of earthquake source, epicenter location, and magnitude

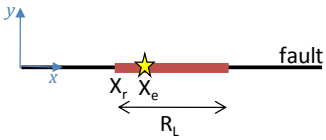

Figure 3: Fault-specific local coordinate system

For a given rupture length, the source-to-site distance (the shortest distance between the site and the rupture) is defined for each site within the source-specific coordinate system (see Figure 4). Suppose that there are J faults (indexed by $j = 1, \ldots, J$) in the region of the infrastructure system. Using the line-source idealization for all faults, the distance between the ith site and a rupture on the jth fault, is computed as

$$R_i = \sqrt{\left(X_{d,i}^j\right)^2 + \left(y_{s,i}^j\right)^2 + \left(z_{s,i}^j\right)^2} \quad (6)$$

where $y_{s,i}^j$ and $z_{s,i}^j$ are the coordinates of site i in the coordinate system defined by source j, and $X_{d,i}^j$ is the x-direction distance between site i and the nearest point on the rupture on source j. For the straight-line idealization of a fault, $X_{d,i}^j$ is expressed using simple geometry as:

$$X_{d,i}^j = \max\left[X_r^j - x_{s,i}^j, x_{s,i}^j - min\left(X_r^j + R_L, F_L^j\right), 0\right] \quad (7)$$

where $x_{s,i}^j$ is the x-direction coordinate of site i and X_r^j is the left end of the rupture, both in the coordinate system defined by source j. The term $\min\left(X_r^j + R_L, F_L^j\right)$ specifies the coordinate of the right end of the rupture. Due to finite fault dimensions, this coordinate is physically constrained to be less than the fault length. For more general geometric configurations, i.e., faults that are not idealized as straight lines, similar expressions can be derived, though they are typically more complicated.

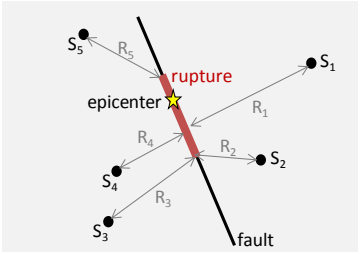

Figure 4: Geographically distributed sites in vicinity of a fault

The BN corresponding to the above description is shown in Figure 5. Node R_i is a child of nodes S_C, R_L, and X_r and is a function of the site coordinates as well. The site coordinates need not be represented in the BN as nodes because they are considered deterministic.

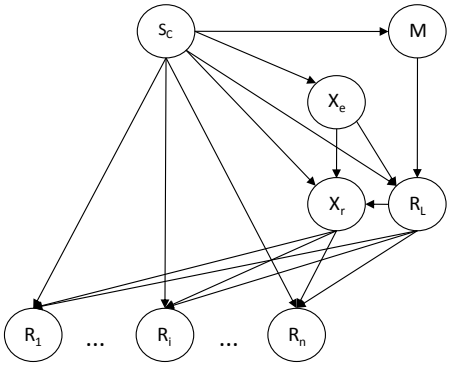

Figure 5: BN modeling source-to-site distance as a function of earthquake source and rupture length and location

Prediction models based on regressions of observed data relate GM intensity at a site to earthquake source and site characteristics, e.g., see Abrahamson et al. (2008). GM prediction equations (also known as attenuation laws) typically have the form

$$\ln S_i = \ln \overline{S}_i + \epsilon_m + \epsilon_{r,i} \quad (8)$$

where $\ln \overline{S}_i = f(M, R_i, \boldsymbol{\theta}_i)$ is the natural logarithm of the median GM intensity at site i expressed as a function of the site-

to-source distance, the earthquake magnitude, and a vector of site/source properties, $\boldsymbol{\theta}_i$, (e.g. faulting mechanism, shear wave velocity, depth to significant impedance contrast). Thus, a node $\ln \overline{S_i}$ is added as a child of nodes M, R_i and S_C. As long as the site properties are taken to be deterministic (or stochastic but unobservable), there is no need to explicitly model them as nodes in the BN. In the above expression, ϵ_m is an inter-event error term and $\epsilon_{r,i}$ is an intra-event error term, both describing variabilities in the logarithmic intensity value relative to the median. Both error terms are zero-mean and normally distributed. The inter-event deviations arise from inaccuracy or idealization in the characterization of the source and represent the variability in GM intensity from earthquake to earthquake. The intra-event deviations arise from uncertain wave propagation and site effects. For a particular earthquake, intra-event deviations represent the variability in the GM intensity from site to site. For a given earthquake, ϵ_m is the same for all sites. As a result, a single node ϵ_m is introduced that is a parent of all site-specific GM intensity nodes. The intra-event errors are site-specific but are spatially correlated. The correlation arises because, for a given earthquake, the magnitude of the difference between the actual and predicted median GM intensity is similar for sites in close proximity to one another but can be less similar as the distance between the sites increases. A node representing $\epsilon_{r,i}$ is added to the BN for each site. The correlation among $\epsilon_{r,i}$'s is modeled with links between all pairs of the corresponding nodes. This is illustrated in Figure 6.

Directivity effects are included in the BN through the addition of a node $f_{d,i}$ representing an amplification factor on GM intensity at site i. In Abrahamson (2000), an amplification factor is added to the natural logarithm of the spectral acceleration from the GM prediction equation. The factor is specified as a function of the amount of the rupture that propagates toward the site and the angle between the direction of the rupture and the site. For this reason, node $f_{d,i}$ is a child of nodes defining the site and source geometry. Additionally, $f_{d,i}$ is affected by the earthquake magnitude and so is a child of node M. Figure 6 shows the complete BN model, including the spatial correlation as well as directivity effects. We refer to the sites for which GM intensity nodes are included in the BN as *ground motion prediction points* (GMPPs).

Monte Carlo simulation is used to compute the CPTs for R_L, X_r, R_i, S_i and other nodes described in the paper, for which the functional dependence between the nodes is known.

4. BN MODELING OF RANDOM FIELDS

Modeling RFs in BNs is computationally demanding. This is because BNs with broadly dependent random variables (densely connected nodes) result in exponential increases in computational demands. This is the case with the nodes representing the intra-event error terms $\epsilon_{r,i}$ in the BN in Figure 6. The increase in computational demand can quickly render the BN computationally intractable for infrastructures with many sites. For this reason we have developed a procedure for modeling the GM intensity RF within the BN framework in a computationally tractable manner.

Define $\epsilon_{r,i} = \epsilon_r(\mathbf{x}_i)$, $i = 1, \ldots, n$ as a set of discrete points in the zero-mean Gaussian RF $\epsilon_r(\mathbf{x})$ describing the spatial distribution of the intra-event error term. This field is defined by a standard deviation function $\sigma_r(\mathbf{x})$ and an autocorrelation function $\rho(\mathbf{x}_i, \mathbf{x}_j)$. Thus the Gaussian vector $\boldsymbol{\epsilon}_r = [\epsilon_{r,1}, \epsilon_{r,2}, \ldots, \epsilon_{r,n}]^T$ has a zero mean vector, standard deviation matrix $\mathbf{D} = diag[\sigma_{r,i}]$ and correlation matrix $\mathbf{R} = [\rho_{ij}]$, where $\sigma_{r,i} = \sigma_r(\mathbf{x}_i)$ and $\rho_{ij} = \rho(\mathbf{x}_i, \mathbf{x}_j)$. The BN representing $\boldsymbol{\epsilon}_r$ is shown in Figure 7. The CPTs in this BN require the specification of the distributions $p(\epsilon_{r,i} | \epsilon_{r,1}, \ldots, \epsilon_{r,i-1}), i = 1, \ldots, n$.

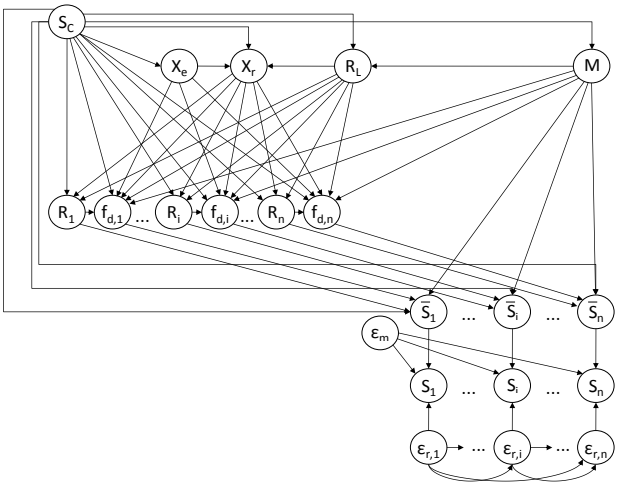

Figure 6: BN modeling GM intensity at each site across a geographically distributed system

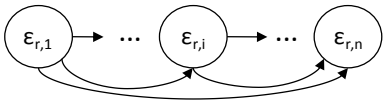

Figure 7: BN modeling points in Gaussian RF

The vector $\boldsymbol{\epsilon}_r$ can be decomposed as a product of an $n \times n$ transformation matrix $\mathbf{T}$ and a $n \times 1$ vector of statistically independent standard normal random variables (RVs) $\mathbf{U}$ as

$$\boldsymbol{\epsilon}_r = \mathbf{TU} = \begin{pmatrix} t_{11} & \cdots & t_{1n} \\ \vdots & \ddots & \vdots \\ t_{n1} & \cdots & t_{nn} \end{pmatrix} \begin{bmatrix} U_1 \\ \vdots \\ U_n \end{bmatrix} \quad (9)$$

The BN corresponding to this transformation is shown in Figure 8. An element of the transformation matrix, t_{ij}, is interpreted as a factor on the link between U_j and $\epsilon_{r,i}$. The covariance matrix is computed as a product of the transformation matrix and its transpose: $\boldsymbol{\Sigma} = \mathbf{TT}'$. It is easy to specify the CPTs required by the BN in Figure 8 because each $\epsilon_{r,i}$ is a deterministic function of the U_i's.

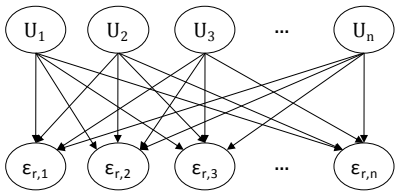

Figure 8: BN showing the transformation $\boldsymbol{\epsilon} = \mathbf{TU}$

The transformation matrix can be determined using the Cholesky factorization, an Eigenvalue (Karhunen–Loève) expansion, or other decomposition methods. The values of the transformation matrix can also be determined approximately via numerical optimization methods, as described later.

While the aforementioned decomposition results in CPTs that are easier to specify than the formulation in Figure 7, it does not decrease computational demand. A reduction in computational demand can be achieved by: (1) reducing the density of links in the BN in Figure 8 and/or (2) reducing the number of states associated with each node (which results in a reduction in CPT sizes, but at the cost of loss of accuracy) We focus here on the reduction of links required to model the random field, which results in the approximation of the spatial error correlation structure. While discretization is not addressed specifically here, the reader is referred to Straub (2009) for additional details on this subject.

Removing a link in the BN corresponds to setting the associated element of the transformation matrix equal to zero. Setting $t_{ij} = 0$ implies removal of the link connecting U_j and $\epsilon_{r,i}$. Define $\hat{\mathbf{T}} = [\hat{t}_{ij}]$ as the matrix $\mathbf{T}$ with some of its elements set to zero. If column i of the transformation matrix has all zero entries, then this implies node U_i has no children and it can be eliminated from the BN. The reduction of nodes/links in the BN results in an approximation of the covariance matrix of $\boldsymbol{\epsilon}_r$. By introducing an additional $n\times1$ vector of statistically independent standard normal RVs $\mathbf{V}$, the approximation in the variances can be eliminated without affecting the covariance (off-diagonal) terms. The addition of these correction terms does not affect the computational efficiency gained through link reduction. Incorporating these correction terms, $\boldsymbol{\epsilon}_r$ is approximated using the transformation

$$\widehat{\boldsymbol{\epsilon}_r} = \mathbf{SV} + \hat{\mathbf{T}}\mathbf{U} = \begin{pmatrix} s_1 & \cdots & 0 \\ \vdots & \ddots & \vdots \\ 0 & \cdots & s_n \end{pmatrix}\begin{bmatrix} V_1 \\ \vdots \\ V_n \end{bmatrix} + \begin{pmatrix} \hat{t}_{11} & \cdots & \hat{t}_{1m} \\ \vdots & \ddots & \vdots \\ \hat{t}_{n1} & \cdots & \hat{t}_{nm} \end{pmatrix}\begin{bmatrix} U_1 \\ \vdots \\ U_m \end{bmatrix} \quad (10)$$

where $\hat{\mathbf{T}}$ is an $n\times m$ $(m \le n)$ transformation matrix, $\mathbf{U}$ and $\mathbf{V}$ are respectively $m \times 1$ and $n\times1$ vectors of statistically independent standard normal RVs, and $\mathbf{S}$ is a diagonal matrix having the elements

$$s_i = \sqrt{\sigma_{r,i}^2 - \sum_{k=1}^{m\le n} \hat{t}_{ik}^2} \quad (11)$$

This formulation ensures that $\hat{\epsilon}_{r,i}$ has the same variance as $\epsilon_{r,i}$. The corresponding BN is shown in Figure 9.

A review of a procedure for determining $\hat{\mathbf{T}}$ is presented here; more details can be found in Bensi et al. (2010a). As described above, setting the elements in the transformation matrix to zero corresponds to a reduction of links. Link reduction may be accomplished by: (1) removing U-nodes and all associated links by setting an entire column of the transformation matrix to zero, (2) selectively removing links while keeping the full number of U-nodes, or (3) first reducing the number of U-nodes and then selectively removing links from the remaining U-nodes. When eliminating nodes and links, the goal is to properly balance computational efficiency and accuracy, i.e., removing as many nodes/links as possible without significantly reducing the accuracy of representing the correlation structure of the RF.

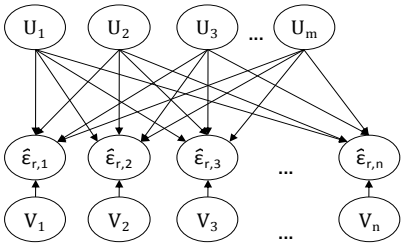

Figure 9: BN corresponding to $\widehat{\boldsymbol{\epsilon}_r} = \mathbf{SV} + \hat{\mathbf{T}}\mathbf{U}$

When using transformation matrices obtained by decomposition methods (e.g. eigenvalue expansion, Cholesky factorization), nodes and links are eliminated as a function of node and link importance measures. The node importance measure (NIM) is defined as

$$M_i = \sum_{k=1}^{n}\sum_{l=k}^{n} |\Delta_i(k,l)| \quad (12)$$

where M_i is the NIM associated with node U_i and $\Delta_i(k,l)$ is the $(k,l)^{th}$ element of the matrix Δ_i, computed as

$$\Delta_i = T_i T_i' \quad (13)$$

where T_i is the i^{th} column of the transformation matrix $\mathbf{T}$ and the prime indicates matrix transpose. Δ_i quantifies the contribution of U_i to the covariance matrix. Thus M_i is a measure of how much of the information contained in the covariance matrix is lost by eliminating U_i. It follows that eliminating the U-node associated with the smallest NIM results in the least loss in accuracy. Similarly, a link importance measure (LIM) associated with each t_{ij} is defined as

$$m_{ij} = \sum_{k=1}^{n}\sum_{l=k}^{n} |\delta_i(k,l)| \quad (14)$$

where m_{ij} is the NIM associated with link t_{ij}, $\delta_{ij}(k,l)$ is the $(k,l)^{th}$ element of the matrix δ_{ij} computed as:

$$\delta_{ij} = T_i T_i' - T_{j,i} T_{j,i}' \quad (15)$$

where T_i is the i^{th} column of the transformation matrix $\mathbf{T}$ and $T_{j,i}$ is i^{th} column of the transformation matrix with the j^{th} element set equal to zero. The links in the BN are ordered by LIM and elimination of the link with the smallest importance measure results in the least loss in accuracy. The node- and link-based approaches can be combined, with U-nodes first eliminated based on NIMs followed by the elimination of links based on LIMs.

Alternatively, the approximate transformation matrix can be defined through an optimization scheme. A node-based elimination approach is defined by first specifying the number of U-nodes to include (m) and then solving the optimization problem

$$\min \sum_{i=1}^{n-1}\sum_{j=i+1}^{n}\left[\rho_{ij} - \frac{\sum_{k=1}^{m\le n} \hat{t}_{ik} * \hat{t}_{jk}}{\sigma_{r,i}\sigma_{r,j}}\right]^2 \quad \text{subject to:} \quad \sum_{k=1}^{m\le n} \hat{t}_{ik}^2 < \sigma_{r,i}^2, \ \forall i \quad (16)$$

where the objective is to minimize the sum of squared

deviations between the actual and approximated correlation coefficients. The use of non-linear constrained optimization to determine the terms of the approximate transformation matrix was suggested by Song & Ok (2009) and Song & Kang (2009).

Analogously, a link-based optimization problem can be formulated in which the number of links is specified rather than the number of nodes. The result is a mixed-integer non-linear constrained optimization problem. It was found that such a formulation performs poorly in practice. Instead, an iterative procedure for link elimination has been developed. First, the optimization described in (16) is performed. Then links are eliminated individually according to their LIM. The values of the remaining links are then re-optimized. The full iterative procedure is described in Figure 10. The iterative procedure can be adapted so that links are eliminated based on magnitude of LIM, i.e. all links with LIMs below a specified threshold are eliminated.

INITIALIZE

1. Specify:
   m = maximum number of U-nodes to include
   N_e = the number of links to eliminate (N_e)
2. Determine the $n \times m$ matrix $\mathbf{T}_0$ with elements obtained by solving the optimization problem in (16)

ELIMINATE LINKS

for $p = 1, \dots, N_e$

1. Calculate LIMs for all elements of $\hat{\mathbf{T}}_{p-1}$
2. Identify indices for the elements in $\hat{\mathbf{T}}_{p-1}$ with the smallest p LIM values
3. Determine the $n \times m$ matrix $\mathbf{T}_p$ by setting all elements corresponding to the indices identified in step 2 equal to zero and solving for the remaining elements using (16)

end

Figure 10: Iterative numerical procedure for determining approximate transformation matrix through link elimination

A numerical study was performed in which a large number of standard infrastructure configurations were considered and different analytical and numerical approaches used to compute the approximate transformation matrix. Configurations were analyzed in which the GMPPs were arranged in a line, circle, grid or cluster formation with different inter-site distances. It was found that the numerical optimization procedures achieved the best trade-off between efficiency and accuracy.

5. COMPONENT PERFORMANCE

Typically, the GMPPs selected in the random field model correspond to locations of components in the infrastructure system. For point-site components, such as relatively short span highway bridges and individual facilities, their performance is predicted as a function of the site-specific GM intensity using fragility functions.

Define a damage index set $k = \{0,1,,\dots,K\}$ such that $k = 0$ corresponds to the intact (no damage) state and $k = K$ corresponds to the most severe damage state considered. A seismic fragility function provides the conditional probability of meeting or exceeding a particular component damage state (DS) k given the GM intensity. Define the fragility of component i for state k as

$$F_k^i(s_i) = \Pr(\text{meeting or exceeding DS } k | S_i = s_i) \quad (17)$$

Note that $F_0^i(s_i) = 1$. The probability that the component is in damage state k is then computed as

$$p_k^i(s_i) = F_k^i(s_i) - F_{k+1}^i(s_i) \quad (18)$$

A node is introduced into the BN representing the state of point-site component i and is labeled C_i. Node C_i has mutually exclusive collectively exhaustive states corresponding to the damage index set. The corresponding BN is shown in Figure 11. The BN shown in this figure makes use of objects represented by rectangles with rounded corners. Behind this object there is a BN modeling seismic demands (as in Figure 6) that is hidden to reduce graphical clutter.

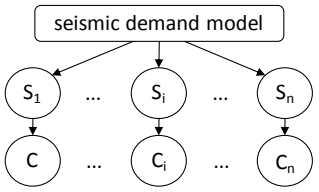

Figure 11: BN modeling performance of point-site components

For distributed components, such as pipelines and rail segments, it is not adequate to model the performance at a single point. Typically, performance functions (analogous to fragility functions) of these linear components are expressed as a mean number of damages of state k or greater per unit length, given a level of GM intensity. The failures along a distributed component are often assumed to follow a Poisson process. One or more failures along the length constitutes failure of the entire component (Adachi & Ellingwood 2008).

While a distributed component may be continuous, the BN requires discretization of the random field and thus distributions of GM intensity are only available at the discrete GMPPs represented by nodes S_i, $i = 1, \dots, n$. As a result, it is necessary to discretize the distributed component into segments. GMPPs modeled in the BN are then selected to correspond with the ends of each segment. Each discretized segment is considered a "component" in the system. Define $C_{i,i+1}$ as the segment between GMPPs represented by nodes S_i and S_{i+1}.

Let $\eta_i^k(s_i)$ be the mean rate of damage points of state k or greater along the component when GM intensity $S_i = s_i$. Associated with the component segment $C_{i,i+1}$ there are two mean damage rates: $\eta_i^k(s_i)$ and $\eta_{i+1}^k(s_{i+1})$. Interpolating linearly between these two values gives the mean damage rate as a function of the coordinate along the component. Assuming damages occur randomly, the probability that the component experiences damage of state k (i.e. the probability of at least one incident of damage of state k) is computed by treating the occurrence of damages as a non-homogenous Poisson process. The mean number of damages of state k or greater for the entire component $C_{i,i+1}$ is then

$$\mu^{\mathrm{k}}_{i,i+1}(s_i, s_{i+1}) = \frac{L_{i,i+1}}{2}\left(\eta^{\mathrm{k}}_{i}(s_i) + \eta^{\mathrm{k}}_{i+1}(s_{i+1})\right) \quad (19)$$

where $L_{i,i+1}$ is the length of $C_{i,i+1}$. The probability that $C_{i,i+1}$ is in damage state k given GM intensity s_i and $s_{i,i+1}$ (expressed $p^k_{i,i+1}(s_i, s_{i,i+1})$) is then be computed as

$$\begin{aligned} p^k_{i,i+1}(s_i, s_{i+1}) &= \exp\left(-\mu^1_{i,i+1}(s_i, s_{i+1})\right) \quad \text{for } k = 0 \\ &= \exp\left(-\mu^{k+1}_{i,i+1}(s_i, s_{i+1})\right) - \exp\left(-\mu^k_{i,i+1}(s_i, s_{i+1})\right), \\ &\quad \text{for } k = 1, \ldots, K-1 \\ &= 1 - \exp\left(-\mu^{\mathrm{K}}_{i,i+1}(s_i, s_{i+1})\right), \text{ for } k = K \end{aligned} \quad (20)$$

The BN corresponding to the above description is shown in Figure 12. The node representing the damage state of component segment $C_{i,i+1}$ is modeled as a child of GM intensity nodes at either end of the segment: S_i and S_{i+1}.

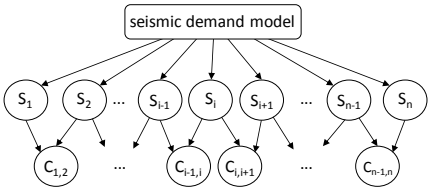

Figure 12: BN modeling performance of discretized segments of a continuous component

6. SYSTEM PERFORMANCE

6.1 Performance of series and parallel systems

The performance of the system is defined as a function of the component damage states. For brevity and simplicity, we focus here on series and parallel systems with binary components. However, BN formulations for more complex system configurations (e.g. general systems with multi-state components) have been developed with an emphasis on computational efficiency and readability (Bensi et al. 2009; Bensi et al. 2010b). Additionally a simple illustrative example is presented to demonstrate how descriptions provided in this paper can be extrapolated to more complex systems. One option for characterizing system performance is to define a single node S_{sys}, which gives the state of the system as a child of all nodes representing the states of the components (a converging structure). For a system with n binary components, node S_{sys} would have a CPT of size 2^n. The exponential growth in the size of the CPT associated with S_{sys} as n increases can quickly render a BN computationally intractable. A more efficient system performance formulation is achieved by constructing chain-like structures that we term failure path sequences (FPSs) and survival path sequences (SPSs). We describe this below for a system with binary component states.

Define a FPS as a chain containing a minimum set of failure events whose joint realization constitutes failure of the system. It is noted that the terms "sequence" and "chain of events" do not have any time-based implications. For a parallel system, there is only one FPS (i.e. all components must fail for the system to fail). For a series system with n components, there are n FPSs (i.e. if any component fails, the system fails). Conversely, a SPS is a chain containing a minimum set of survival events whose joint realization constitutes system survival. A series system has one SPS while a parallel system as n SPSs. Readers familiar with classical systems analysis will recognize the connection between FPSs and minimum cuts sets as well as SPSs and minimum link sets.

A FPS is comprised of a chain of failure path events (FPEs), each of which gives the state of the chain up to that event. Let $E_{f,i}$ be a node representing the FPE associated with component i. Node $E_{f,i}$ has two states: failure (state 0) and survival (state 1). The state of $E_{f,i}$ is as a function of the states of associated component i and the previous FPE in the FPS. The state of $E_{f,i}$ is expressed as

$$\begin{aligned} E_{f,i} &= 0 \text{ if } E_{f,i-1} = 0 \text{ and } C_i \text{ has failed} \\ &= 1 \text{ otherwise} \end{aligned} \quad (21)$$

Thus, for a parallel system, the BN system formulation takes the form shown in Figure 13. The state of node $E_{f,1}$ is equal to the state of node C_1. $E_{f,2}$ is in failed state only if the previous FPE $E_{f,1}$ is in failed state and C_2 is in failed state. This pattern continues such that $E_{f,n}$ is in failed state only if both $E_{f,n-1}$ and C_n are in failed state. Thus, the state of $E_{f,n}$ gives the state of the system, which is shown by node S_{sys} being a child of $E_{f,n}$.

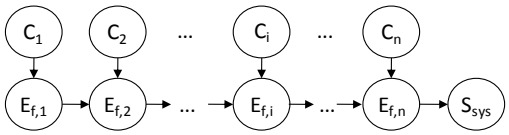

Figure 13: BN using FPEs to define a parallel system

For a series system, the BN formulation using FPSs is shown in Figure 14. As can be seen, there are n FPSs, each of which is defined by one FPE. Thus, the size of the CPT associated with the S_{sys} is 2^n and there is no computational advantage to this approach. As shown below, a more efficient formulation is achieved by using SPSs.

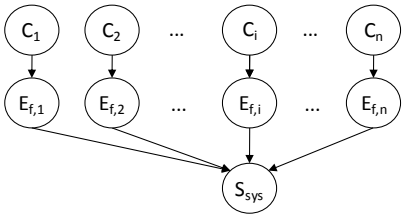

Figure 14: BN using FPEs to define a series system

A SPS is comprised of a chain of survival path events (SPEs), each of which gives the state of the chain up to that event. The state of each SPE is defined as a function of an associated component and the previous SPE in the SPS. Thus, the state of $E_{s,i}$ is defined as

$$\begin{aligned} E_{s,i} &= 1 \text{ if } E_{s,i-1} = 1 \text{ and } C_i \text{ has survied} \\ &= 0 \text{ otherwise} \end{aligned} \quad (22)$$

Where $E_{s,i} = 1$ indicates that node $E_{s,i}$ is in survival state and $E_{s,i} = 0$ indicates failure. Thus, for a series system, the BN system formulation takes the form shown in Figure 15. The state of node $E_{s,1}$ is equal to the state of node C_1. $E_{s,2}$ is in survival state only if $E_{s,1}$ is in survival state and C_2 is in survival state. This pattern continues such that $E_{s,n}$ is in survival state only if both $E_{s,n-1}$ and C_n are in survival state. Consequently, the state of $E_{s,n}$ gives the state of the system.

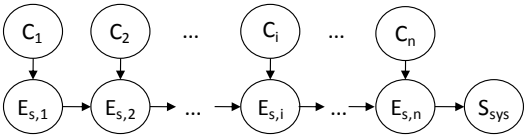

Figure 15: BN formulation using SPEs to define a series system

For more complex systems, a more sophisticated approach has been developed but is not detailed in this paper (see Bensi et al. 2009; Bensi et al. 2010b).

6.2 Example Application

Consider the simple infrastructure system in Figure 16 located parallel to a 120km long fault and consisting of distributed components (lines) and point-site components (squares). The coordinates of the GMPPs (represented by numbered circles) in the fault-specific coordinate system are indicated on the figure. System survival is defined as the event in which there is connectivity between the source and sink. The direction of flow through the network is indicated by arrows.

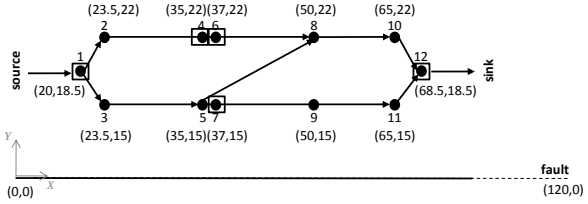

Figure 16: Example infrastructure system

Seismic demands on the system are modeled using the previously described GM intensity RF BN using the Campbell & Bozorgnia (2006) GM prediction equation. The magnitude distribution is based on a characteristic earthquake model. Wells and Coppersmith (1994) defines the magnitude-rupture length relationship. The spatial error correlation model is taken from Park et al. (2007). The performance of the point-site (PGA-sensitive) and distributed (PGV-sensitive) components is modeled as described in section 5 using damage functions adapted from HAZUS-MH. The performance of the system is modeled by extension of the previously described parallel and series system formulations. This example is presented for illustrative purposes to demonstrate the development of a systems analysis BN for non-parallel/series systems and to show the power of using the BN for information updating. The model assumptions are not restrictive and can easily be changed based on the knowledge and preferences of the modeler.

Let $C_{d,i,j}$ represent the distributed component between GMPPs i and j. Let $C_{p,k}$ be the point-site component located at GMPP k. There are three survival path sequences (minimum link sets) for this system. The components associated with the SPEs in the SPSs are:
$\{C_{p,1}, C_{d,1,2}, C_{d,2,4}, C_{p,4}, C_{d,4,6}, C_{p,6}, C_{d,6,8}, C_{d,8,10}, C_{d,10,12}, C_{p,12}\}$, $\{C_{p,1}, C_{d,1,3}, C_{d,3,5}, C_{d,5,8}, C_{d,8,10}, C_{d,10,12}, C_{p,12}\}$, $\{C_{p,1}, C_{d,1,3}, C_{d,3,5}, C_{d,5,7}, C_{p,7}, C_{d,7,9}, C_{d,9,11}, C_{d,11,12}, C_{p,12}\}$.

There are many ways to formulate a system analysis BN for this example using different orderings of the SPEs/FPEs of SPSs/FPSs. Figure 17 presents a BN formulation in which SPE nodes are arranged in three distinct chains, each corresponding to one SPS. Because multiple SPEs are associated with some of the components, an additional superscript index is added to the SPE nodes. In Figure 17, the performance of the overall system is represented by node S_{sys} with its state defined as

$$S_{sys} = \bigcup_{i=1}^{3} E_{S,12}^{(i)} \tag{23}$$

where S_{sys} is the event in which the system survives and $E_{s,12}^{(i)}$ represents the ith SPE associated with component 12.

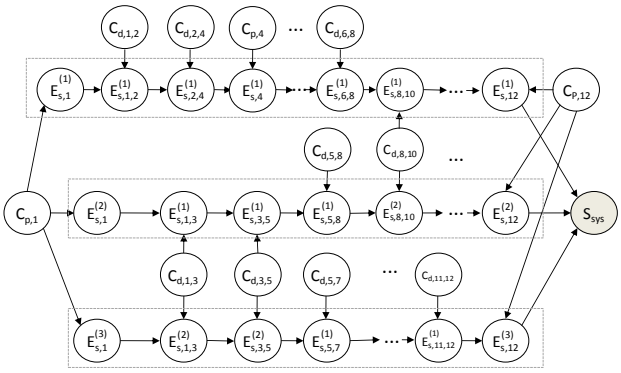

Figure 17: BN model for example system

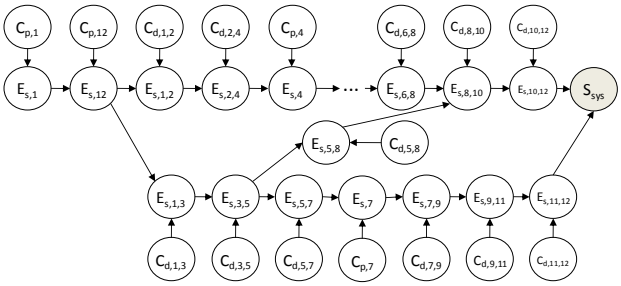

Figure 18: Improved BN model for example system

The number of SPE nodes in the BN can be reduced through careful structuring. The order in which SPE nodes are chained together to create SPSs must be optimized to minimize computational demand. The optimization is subject to the requirement that all SPSs are included and no artificial SPS is introduced that is not present in the actual system. Additional details on optimizing the arrangement of SPEs/FPEs to create SPSs/FPSs in system analysis BNs can be found in Bensi et al (2010b). For this example, Figure 18 presents an improved system analysis BN in which the order of SPE nodes is such that there is only one SPE associated with each component.

To illustrate the value of the BN framework for information updating, we show the effect of different post-earthquake evidence scenarios on the system and component failure probabilities. The following post-earthquake evidence cases (ECs) are considered:

(1) A magnitude 6.8 earthquake has occurred with epicenter located 30km from left end of the fault

(2) EC (1) + PGV at GMPP 3 is measured to be 23cm/sec.

(3) EC (2) + component $C_{d,6,8}$ is observed to have failed.

(4) EC (2) + component $C_{d,6,8}$ is observed to have survived.

Table 1 contains component and system failure probabilities for each EC. Note that the probabilities change with different ECs. Particularly, observe that evidence on the

intensity at a GMPP or the performance of a component has the greatest impact on the failure probabilities of near-by components due to RF effects. Evidence on the performance of a component propagates through the BN by updating the distribution of the GM intensity at the location of the component. This in turn updates the full GM intensity RF model and provides revised distributions of GM intensities at other locations. The updated GM distributions then change the failure probabilities of associated components. As more observations become available, the model "infers" the true value of unobservable parameters (e.g. the values of the inter- and intra-event deviations or the location of the rupture, which is not commonly known immediately following an earthquake) with increasing accuracy. Thus, we have a probabilistic framework that combines observations and physical models to provide an up-to-date characterization of the system.

Table 1: Failure probabilities (%) for example system

	EC(1)	**EC(2)**	**EC(3)**	**EC(4)**
$C_{p,1}$	4.5	8.1	9.0	8.0
$C_{d,1,2}$	2.7	4.3	4.7	4.3
$C_{d,1,3}$	3.8	7.9	8.1	7.9
$C_{d,2,4}$	5.0	6.5	8.1	6.4
$C_{d,3,5}$	9.7	17.0	18.3	16.9
$C_{d,4,6}$	0.9	1.0	1.6	1.0
$C_{p,4}$	3.2	3.9	6.2	3.7
$C_{d,5,7}$	1.8	2.1	2.7	2.1
$C_{d,5,8}$	10.2	11.5	15.8	11.3
$C_{p,6}$	2.6	3.1	5.9	2.9
$C_{d,6,8}$	5.4	6.2	100	0.00
$C_{p,7}$	6.6	7.8	10.3	7.6
$C_{d,7,9}$	10.4	11.8	14.7	11.6
$C_{d,8,10}$	5.5	6.2	8.9	6.1
$C_{d,9,11}$	9.6	10.9	13.1	10.7
$C_{d,10,12}$	1.8	2.1	2.4	2.1
$C_{d,11,12}$	2.4	2.7	3.1	2.7
$C_{p,12}$	2.2	2.7	3.2	2.6
System	**12.05**	**18.91**	**39.82**	**17.53**

7. SOLVING DECISION PROBLEMS

To solve decision problems, a BN can be extended by decision and utility nodes. Once these nodes have been added to a BN, the new graph is called an *influence diagram* (ID). An ID encodes both the probability model and the decision problem structure. A decision node is represented by a rectangle and is defined by a finite set of states corresponding to decision alternatives. Links going into a decision node, referred to as *information links*, indicate that the states of the parent nodes are known prior to deciding. A utility node is represented by a diamond. Utility nodes have no states; instead they are assigned a utility value (e.g. monetary units) as a function of the states of their parents. The optimal decision alternative is the one that maximizes expected utility. Additional details on influence diagrams can be found in Jensen & Nielson (2007).

For simplicity, in this paper, we explain IDs by an example. Consider a post-earthquake scenario in which an earthquake has occurred and placed a seismic demand on a facility. The owner must decide whether to inspect the facility (for which a cost will be incurred) and then decide whether to shut it down (with or without first making an inspection). The decision to shut down the facility must be made under competing objectives: the owner does not want to incur a liability by making an unsafe decision (i.e. keep the facility open when it is damaged) nor lose revenue by unnecessarily shutting down the facility. The ID modeling this decision problem is shown in Figure 19. Different IDs can be constructed for this simple problem based on the preferences and practices of the decision-maker. The following notation is used: S= seismic demand, D_{true} = true damage state of the facility (e.g. heavily damaged, slightly damaged, no damage), D_{obs} = observed component damage state based on an inspection, C_I = inspection cost, L = liability for making an unsafe decision to continue operation of the facility when it is damaged, R = lost revenue due to shutting down the facility, $Inspect?$= the inspection decision (e.g. no inspection, visual inspection, extensive inspection), $Shut\text{-}down?$= decision to shut-down the facility.

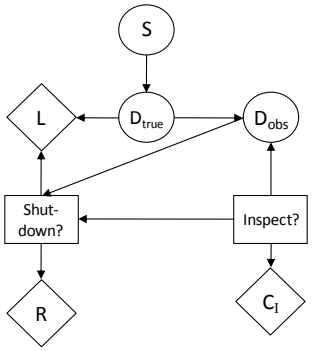

Figure 19: ID corresponding to inspection/close decision

In Figure 19, the true damage state of the component is a function of the seismic demand. The true component damage state is assumed to be a latent variable but it can be known with less uncertainty depending on the inspection type selected, e.g. the true damage state of the component may be known with (near) perfect certainty if an extensive inspection is performed, but with less certainty if only a visual inspection is performed. Of course, no information is gained if an inspection is not performed. Node D_{obs} represents the damage state observed during the inspection. The "inspection-quality" relationship between observed and actual damage is encoded in the ID with node D_{obs} being a child of node D_{true} and the inspection decision. Observations are entered in node D_{obs} and based on the inspection type, this evidence probabilistically updates the damage probabilities for node D_{true}. Associated with the inspection choice is a cost, which will increase as the inspection quality improves. This is modeled by a utility node that is functionally dependent on the inspection decision node. It is assumed that the inspection decision and associated outcome (if an inspection is made) are known before a decision is made regarding facility shut-down. This is indicated by information links between nodes $Inspect?$ and D_{obs} and node $Shut\text{-}down?$. When working with IDs, defining the order of

decisions is important. Defining this order encodes the value of information obtained by performing the inspection. As a function of the closure decision and the true damage state of the facility, there is a utility node that represents the liability incurred when making an unsafe decision. Note that this liability is a function of the true damage state, not the observed damage state. There is an additional utility node dependent on the shut-down decision node, which represents the loss incurred when the facility is not operating. Thus, the two utility nodes represent the competing objectives to maintain operability and not incur a liability.

For more complex decision problems relating to geographically distributed infrastructure systems, the GM demands are modeled as a spatially distributed RF with component specific intensity nodes. Component performance is modeled as described in section 5. System performance is modeled consistent with the procedure outlined in section 6. Typically, the utility node representing lost revenue is associated with system failure rather than component failure. Thus, we take into account the importance of a component to the entire system and its likelihood of damage when deciding whether to shut it down.

As information evolves in near-real time following an earthquake, observations of GM intensity, component performance, and system response are entered into the BN. As decisions are made, the choices are also entered into the BN. This information propagates through the BN to provide an up-to-date characterization of the probability model and decision structure. Thus, the ID provides the decision-maker with guidance on optimal decisions at any point in time, based on all the available information.

8. CONCLUSIONS

A broad overview of a BN-based framework for aiding near-real time post-earthquake decision-making is presented. It is shown that BNs are particularly well-suited for the proposed application, but like other computational tools, they are not without limitations. We have detailed some of our efforts to address these limitations and make BNs a viable tool for infrastructure risk assessment and management. It has also been shown that the facility of information updating makes BNs an excellent tool for near-real time risk management and decision-support.

Acknowledgements:

The authors acknowledge research support from the Pacific Earthquake Engineering Research (PEER) center Transportation Systems Research Program.

References:

Abrahamson, N.A., 2000. Effects of rupture directivity on probabilistic seismic hazard analysis. In *Proceedings of the 6th International Conference on Seismic Zonation, Palm Springs, Earthquake Engineering Research Institute*.

Abrahamson, N. et al., 2008. Comparisons of the NGA Ground-Motion Relations. *Earthquake Spectra*, 24(1), 45-66.

Adachi, T. & Ellingwood, B.R., 2008. Serviceability of earthquake-damaged water systems: Effects of electrical power availability and power backup systems on system vulnerability. *Reliability Engineering & System Safety*, 93(1), 78-88.

Bensi, M., Straub, D. & Der Kiureghian, A., 2010a. Bayesian network modeling of correlated random variables drawn from a Gaussian random field. *Article in Preparation*.

Bensi, M., Straub, D. & Der Kiureghian, A., 2010b. Efficient Bayesian network formulations for modeling system performance (forthcoming). In *Proceedings of IFIP working group 7.5 on Reliability and Optimization of Structural Systems*. Munich, Germany.

Bensi, M., Straub, D., Friis-Hansen, P. & Der Kiureghian, A., 2009. Modeling infrastructure system performance using BN. In *Proceedings of the 10th International Conference on Structural Safety and Reliability*. Osaka, Japan.

Campbell, K. & Bozorgnia, Y., 2007. *Campbell-Bozorgnia NGA Ground Motion Relations for the Geometric Mean Horizontal Component of Peak and Spectral Ground Motion Parameters*, University of California, Berkeley: Pacific Earthquake Engineering Research Center.

Department of Homeland Security, Emergency Preparedness and Response Directorate, *HAZUS-MH MR4 Technical Manual*, Washington D.C.: FEMA, Mitigation Division.

Hugin Expert, *Hugin Ressearcher*, Denmark. Available at: www.hugin.com.

Jensen, F.V. & Nielson, T.D., 2007. *Bayesian Networks and Decision Graphs* second., New York: Springer Science Business Media|Springer.

Langseth, H. et al., 2009. Inference in hybrid Bayesian networks. *Reliability Engineering & System Safety*, 94(10), 1499-1509.

Lauritzen, S., 1992. Propagation of probabilities, means and variances in mixed graphical association models. *Journal of the American Statistical Association*, 87, 1098-1108.

Lauritzen, S.L. & Jensen, F., 2001. Stable local computation with conditional Gaussian distributions. *Statistics and Computing*, 11(2), 191-203.

Lauritzen, S.L. & Nilsson, D., 2001. Representing and Solving Decision Problems with Limited Information. *Management Science*, 47(9), 1235-1251.

Park, J., Bazzurro, P. & Baker, J.W., 2007. Modeling spatial correlation of ground motion Intensity Measures for regional seismic hazard and portfolio loss estimation. In T. Kanda, ed. *Applications of Statistics and Probability in Civil Engineering*. Tokyo, Japan: Taylor & Francis Group.

Song, J. & Kang, W., 2009. System reliability and sensitivity under statistical dependence by matrix-based system reliability method. *Structural Safety*, 31(2), 148-156.

Song, J. & Ok, S., 2009. Multi-scale system reliability analysis of lifeline networks under earthquake hazards. *Earthquake Engineering & Structural Dynamics*. Available at: http://dx.doi.org/10.1002/eqe.938 [Accessed January 6, 2010].

Straub, D., 2009. Stochastic Modeling of Deterioration Processes through Dynamic Bayesian Networks. *Journal of Engineering Mechanics*, 135(10), 1089-1099.

Wells, D. & Coppersmith, K., 1994. New Empirical Relationships among Magnitude, Rupture Length, Rupture Width, Rupture Area, and Surface Displacement. *Bulletin of the Seismological Society of America*, 84(4), 974-1002.